https://doi.org/10.5194/egusphere-2026-296
Preprint. Discussion started: 3 February 2026

Absence of nitrogen threshold effect on soil respiration leads to an underestimation of global soil carbon sequestration in model

Daju Wang[1,9,#], Ruowen Yang[2,#], Lei Cai[2,#], Pierre Gentine[3,4], César Terrer[5], Shuli Niu[6,7], Mirco Migliavacca[8], Wenping Yuan[9,10], Ryunosuke Tateno[11], Junlan Xiao[1], Josep Peñuelas[12,13], Caixian Tang[14], Yongshuo H. Fu[15], Weiyu Shi[1,*]

[1]Chongqing Jinfo Mountain Karst Ecosystem National Observation and Research Station, School of Geographical Sciences, Southwest University, Chongqing, 400700, China
[2]Department of Atmospheric Sciences, Yunnan University, Kunming, 650000, China
[3]Department of Earth and Environmental Engineering, Columbia University, New York, 10027, USA
[4]Center for Learning the Earth with Artificial Intelligence and Physics (LEAP), Columbia University, 10027, New York, USA
[5]Department of Civil and Environmental Engineering, Massachusetts Institute of Technology, Cambridge, 02139, USA
[6]Key Laboratory of Ecosystem Network Observation and Modeling, Institute of Geographic Sciences and Natural Resources Research, Chinese Academy of Sciences, Beijing, 100101, China
[7]College of Resources and Environment, University of Chinese Academy of Sciences, Beijing, 101408, China
[8]European Commission, Joint Research Centre (JRC), Ispra, 21027, Italy
[9]School of Atmospheric Sciences, Guangdong Province Data Center of Terrestrial and Marine Ecosystems Carbon Cycle, Sun Yat-sen University, Zhuhai, 519000, China
[10]Sino-French Institute for Earth System Science, College of Urban and Environmental Sciences, Peking University, Beijing, 100871, China
[11]Field Science Education and Research Center, Kyoto University, Kyoto, 113-8656, Japan
[12]CREAF, Cerdanyola del Vallès, Catalonia, 08290, Spain
[13]CSIC, Global Ecology Unit, CREAF-CSIC-UAB, Cerdanyola del Vallès, 08290, Spain
[14]La Trobe Institute for Sustainable Agriculture and Food, Department of Animal, Plant & Soil Sciences, Bundoora, VIC, 3083, Australia
[15]College of Water Sciences, Beijing Normal University, Beijing, 100875, China
[#]These authors contributed equally to this work.

Correspondence to: Weiyu Shi (shiweiyu@swu.edu.cn)

Abstract. Soil respiration (*Rs*), a key component of the global carbon cycle, plays a pivotal role in regulating atmospheric CO_2 concentrations and climate. Yet, the global responses of *Rs* and its components, including heterotrophic respiration (*Rh*) and autotrophic respiration (*Ra*) to varying levels of nitrogen (N) deposition remain poorly understood. By synthesizing global data from 931 paired observations of 226 experimental sites, this study indicated that *Rs* responses generally decline with increasing N inputs: low to moderate additions exert negligible or slightly positive effects, while higher additions consistently suppress *Rs*, mainly through reductions in *Rh*. Based on an N addition threshold (N_{th}) that indicates whether *Rs* increases or decreases, we incorporated this response pattern into the Community Land Model version 5 (CLM5). We demonstrate that ignoring N's variable impacts may cause *Rs* to be overestimated or soil carbon sequestration to be underestimated by up to 20%. Our results provide a robust global assessment of *Rs*-N relationships and demonstrate the importance of representing N-induced reductions in soil respiration in Earth system models, to improve predictions of terrestrial carbon-climate feedbacks.

https://doi.org/10.5194/egusphere-2026-296
Preprint. Discussion started: 3 February 2026

1 Introduction

Soil respiration (*Rs*), the flux of autotrophically- and heterotrophically-generated CO_2, emits 10 times CO_2 to the atmosphere than fossil fuels annually (Bond-Lamberty & Thomson, 2010). As the second largest carbon flux from terrestrial ecosystems to the atmosphere (Raich & Schlesinger, 1992), *Rs* is critical to the global soil carbon budget and the accurate projection of the future climate change (Xu & Shang, 2016). With increasing nitrogen (N) deposition, global *Rs* dynamics and soil carbon stock changes remain unclear. Increasing evidence from N addition experiments and global meta-analysis has revealed diverse responses of *Rs* to N addition (Lu et al., 2011; Lu et al., 2021; Magnani et al., 2007; Zhou et al., 2014; Zhong et al., 2016; Yang et al., 2022; Liu et al., 2023). The pattern of variations in *Rs* along the N addition gradients has been progressively unveiled across diverse sites, suggesting that the impacts of N addition on *Rs* are expected to be largely dose-dependent (Lee & Jose, 2003; Raposo et al., 2020; Tian et al., 2016a). However, global comprehension of how *Rs* respond to diverse levels of N addition remains ambiguous (Deng et al., 2020; Zhou et al., 2014; Zhou et al., 2016).

Moderate N additions can alleviate soil N limitation and promote plant growth. However, when the input exceeds the retention capacity (of both soil and vegetation), N saturation is reached, and leaching occurs (Aber et al., 1998; Chiwa et al., 2019). Nitrogen saturation also leads to reductions in microbial biomass and activity (Lee and Jose, 2003; Treseder, 2008), soil acidification (Wang et al., 2019a), changes to belowground carbon distribution, and potential harm to the plant root systems (Janssens et al., 2010). Global evidence of N saturation of above-ground net primary productivity in terrestrial ecosystems has been proposed, with an N saturation flux threshold of 5–6 g m^{-2} yr^{-1} (Tian et al., 2016b). Previous studies also suggest a potential saturation threshold for N addition (N_{Th}) for *Rs*, which differentiates the responses of *Rs* to varying N levels. Although numerous N addition experiments have demonstrated the dependence of *Rs* on N addition level (Chen and Chen, 2023; Wang et al., 2019b), the quantification of N addition threshold for *Rs* remains inadequately addressed. Identifying and assigning an appropriate N saturation threshold can enhance our understanding of the responses of *Rs* to N addition (Yu et al., 2018). With the anthropogenic N inputs continued increasing, consideration of the impacts of N saturation on the global carbon cycle can help improve the accuracy of assessments of soil carbon sequestration capacity. Given the spatial heterogeneity of the N limit, the observed evidence should be incorporated into the Earth system models for better accounting for the spatial and temporal patterns of N-induced *Rs* and better future carbon dynamics projections (Niu et al., 2016; Penuelas, 2023; Thomas et al., 2013).

Several process-based and empirical models have been used to estimate the global distribution of N deposition (Schwede et al., 2018) and its potential effects on ecosystems (De Marco et al., 2014; Lamarque et al., 2005; Payne et al., 2017), providing comprehensive estimates of atmospheric N deposition compared to regional monitoring networks (Schwede et al., 2018). With a process-based model, Kicklighter et al. (2019) found a strong control of N on carbon stocks in northern Eurasian forests under different future climate scenarios (Representative Concentration Pathways (RCPs) 4.5 and 8.5). To better understand the effects of global N deposition on *Rs*, Chen and Chen (2023) established linear mixed-effect models by correlating observations with key drivers of *Rs* response to N addition, such as N deposition levels and climatic conditions. However, despite these efforts, estimating soil carbon dynamics under N deposition still has substantial uncertainties. Current Earth

https://doi.org/10.5194/egusphere-2026-296
Preprint. Discussion started: 3 February 2026

system models do not consider the saturation impact of N on *Rs*, resulting in bias of global carbon storage projections (Lee and Jose, 2003; Raposo et al., 2020; Tian et al., 2016a). With global economic activity continuing to increase, it is essential to reduce uncertainty in future carbon sequestration in terrestrial ecosystems through better characterization of the interaction between the amount of change of active N inputs and ecosystem carbon dynamics (Reay et al., 2008).

To that end, this study seeks to improve the representation of *Rs* and soil organic carbon (SOC) under N deposition by incorporating N saturation effects into an Earth system model. Using a global dataset of N addition experiments, we first identified a global mean N addition threshold through multiple algorithms. This threshold, which marks a significant shift in the trend of *Rs* responses along the N addition gradient, was used as a reference parameter to inform improvements in the Community Land Model version 5 (CLM5). Subsequently, we analysed how *Rs* and its components respond across the N addition gradient. Finally, based on the observed N_{Th}, the soil decomposition module in CLM5 was modified to involve the response of *Rs* to N deposition and to predict global soil carbon dynamics, in the 21st century under the latest climate projection scenario of the sixth Coupled Model Intercomparison Project (CMIP6).

2 Materials and Methods

2.1 Data collection and screening for meta-analysis

To perform a meta-analysis, 226 peer-reviewed papers published during the past decades were retrieved by searching the Web of Science, Google Scholar, and the China National Knowledge Infrastructure (CNKI, https://www.cnki.net/) using the following terms: “carbon emission”, “fertilization”, “heterotrophic respiration”, “N addition”, “N deposition”, and “soil respiration”. The N addition in this study only includes the treatment of fertilization or simulated N deposition. In order to ensure the data were appropriate for our analyses, we selected studies that only matching the following criteria. (1) Studies measured at least one pair of variables (soil respiration or environmental variables) in both the control and treatment(s); (2) Selection of N addition experiments performed under the same meteorological conditions, to control for unmeasured factors; (3) *Rs*, *Rh*, and *Ra* (from plant roots and autotrophic microorganisms) were measured using in-situ field experiments; (4) Only records involving N-only addition treatments were retained. Studies with combined treatments (e.g., N+P, N+warming) were excluded. (5) Only experiments that applied N in inorganic forms (e.g., NH_4NO_3) were included, and those using organic forms such as urea were excluded. (6) Croplands were excluded for two main reasons. First, experimental N inputs in croplands are primarily applied in the form of fertilizers (e.g., urea) (Shukla et al., 2017; Liang et al., 2019), which cannot be equated with atmospheric N deposition under natural conditions. Second, due to long-term intensive fertilization, cropland soils exhibit markedly reduced sensitivity to additional N inputs, and their N thresholds (N_{th}) are often much higher than those of other ecosystems (Zhou et al., 2014; Lamptey et al., 2018). Therefore, including croplands in the analysis could introduce systematic bias into global threshold estimates. (7) The means, standard deviations or errors of corresponding variables and sample sizes for control and treatment groups could be directly obtained from the text and/or tables, or from digitized graphs; (8) For soil

https://doi.org/10.5194/egusphere-2026-296
Preprint. Discussion started: 3 February 2026

properties, measured or average measured values were provided for the upper soil layer (0-10 cm); (9) When an experiment reported multiple levels of N addition, we treated each level as one treatment.

We extracted the variables, as shown in Table S1, from these peer-reviewed articles, and collected the data of plant photosynthesis, microbial diversity, and soil enzyme activities under N addition from other published meta-analyses (Table S1). In total, 931 paired observations from 226 experimental sites were extracted (Dataset S1). The ranges of latitudes were from 43.66°S to 64.75°N (Fig. 1).

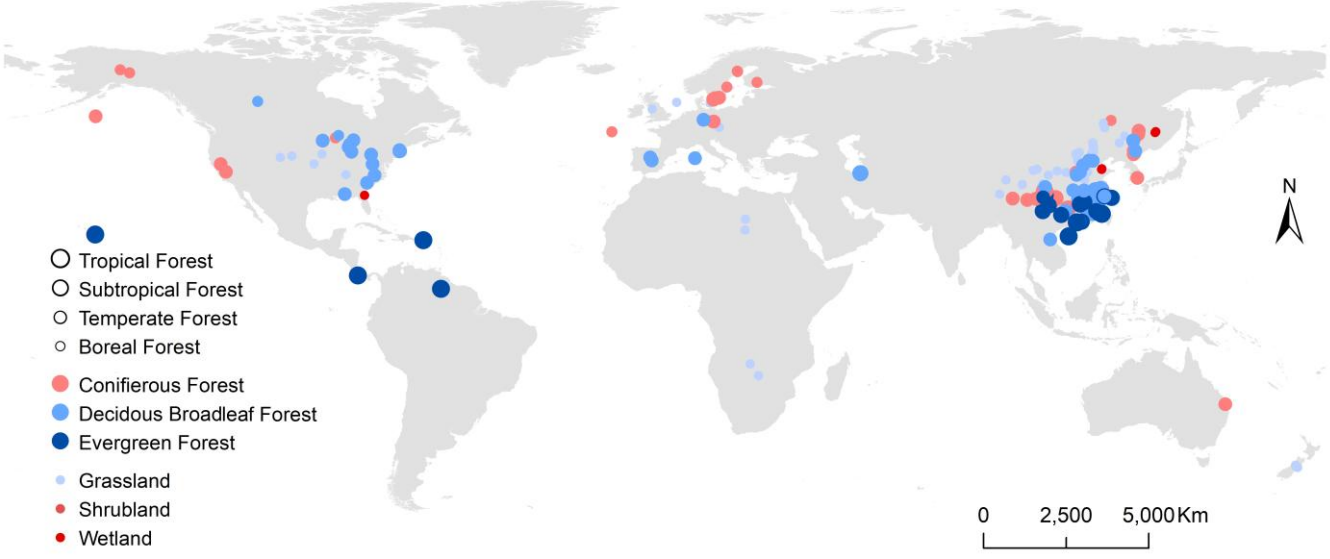

Figure 1: Spatial distribution of N addition experiments included in the meta-analysis.

2.2 Meta-analysis

To calculate the response ratio (*RR*) of each N addition experiment, we took the natural logarithm (ln) of the ratio of treatment to control values for each response variable, as

$$RR = \ln\left(\frac{\bar{X}_t}{\bar{X}_c}\right) = \ln(\bar{X}_t) - \ln(\bar{X}_c) \quad (1)$$

where X_t and X_c are the mean values of a given variable in the treatment and control groups, respectively. Taking the logarithm can linearize the metric, treating deviations in the numerator the same as deviations in the denominator, and significantly reducing skewness in small-sample distributions (Hedges et al., 1999).

While *RR* represents the response ratio of individual pairwise comparisons between treatment and control, the mean weighted response ratio (RR_{++}) was calculated from *RR* to determine regional and global averages as Eq. (2).

$$RR_{++} = \frac{\sum_{i=1}^{m} w_i RR_i}{\sum_{i=1}^{m} w_i} \quad (2)$$

https://doi.org/10.5194/egusphere-2026-296
Preprint. Discussion started: 3 February 2026

where m is the number of experiments in the group (e.g., a geographical region), and RR_i and w_i (i = 1, 2, …, m) are the RR and weight of the i_{th} experiment in the group, respectively. The weights were calculated as $w_i=1/v_i$, where v_i is the within-study variance of study (i). v_i was calculated following Eq. (3).

$$v = \frac{s_t^2}{n_t \bar{x}_t^2} + \frac{s_c^2}{n_c \bar{x}_c^2} \quad (3)$$

where n_t and n_c are the numbers of replicates for the N addition treatment and the control, respectively; and S_t and S_c are the standard deviations for the treatment and control groups, respectively. Some studies did not report the standard deviations; to address this gap, we first calculated the coefficient of variation (CV=standard deviation/mean) using the subset of studies that reported both mean and standard deviation. Then computed the average CV within each dataset, stratified by sub-ecosystem, under the assumption that the relative variability of similar measurements within the same ecological context is comparable. For those studies lacking standard deviation, we estimated the missing values by multiplying the reported mean by the corresponding average CV (Bai et al., 2013).

The RR and variance of a single study were calculated using the *escalc* function from the *R* package *metafor* (Viechtbauer, 2010), and the RR_{++} was calculated in a weighted, mixed-effects model using the rma.mv function in *metafor*, with "study" as a random effect to account for the non-independency of multiple observations in the same study (Terrer et al., 2021). The effect sizes of the N addition treatments were expressed as percentages:

$$Effect\ size = [\exp(RR_{++}) - 1] \times 100\% \quad (4)$$

2.3 Identification of N addition threshold

This study aims to reveal the saturation response pattern of N on *Rs* and to calibrate the Earth system model. To achieve this, we require a calibration parameter that could capture the critical shift in *Rs* response (*RRs*) to N enrichment. In this study, we identify the N addition threshold—a value that characterizes the significant change in *RRs* to N addition—as the calibration parameter. We first calculated the weighted response ratio (RR_{++}) for each N addition level and found that RR_{++} exhibits a decreasing trend as N input increases (Fig. 2a). Therefore, the threshold can be determined by identifying the point at which RR_{++} significantly declines. Subsequently, we applied three change-point detection methods—the sliding t-test (Basseville and Nikiforov, 1195), Pettitt test (Pettitt, 1979), and Mann-Kendall test (Mann, 1945; Kendall, 1975) on the RR_{++} series to determine the specific inflection point (i.e., N addition threshold, N_{Th}) with the highest confidence level.

The sliding t-test is based on the student's t-test, which examines whether the difference in the mean values between two series was significant to identify the abrupt change. The difference was calculated as Eq. (5):

$$t = \frac{\overline{x_1} - \overline{x_2}}{s\left(\frac{1}{n_1} + \frac{1}{n_2}\right)} \quad (5)$$

where x_1 and x_2 are two series of the RR_{++} series, one before and one after a certain point, with sample sizes n_1 and n_2, respectively. The overbar denotes the mean value. And s was calculated as:

https://doi.org/10.5194/egusphere-2026-296
Preprint. Discussion started: 3 February 2026

$$s = \sqrt{\frac{(n_1-1)s_1^2+(n_2-1)s_2^2}{n_1+n_2-2}} \quad (6)$$

where s_1 and s_2 represent the variance of x_1 and x_2. Here, the statistical variable t satisfies the t-distribution with (n_1+n_2–2) degrees of freedom. Given the significance level α, if $|t| > t_\alpha$, the mean value difference between x_1 and x_2 is statistically significant, suggesting an abrupt change of the RR_{++} series at that certain point. We have performed sliding t-tests on multiple points with various subsequence lengths and took the abrupt change with the highest confidence as the threshold.

The Pettitt algorithm is a non-parametric test used to detect change points in time series data (Pettitt, 1979). Its core principle is to compare each data point in the series with all preceding data points to evaluate their relative magnitudes, thereby determining whether a change point exists. Specifically, the algorithm computes a test statistic U_t at each point. If U_t at a certain point is significantly higher than at other positions, that point is considered a likely change point. For a dataset X with N observations, the test statistic U_t was calculated as follows:

$$U_t = U_{t-1} + V_t, t \in [2, N] \quad (7)$$

$$V_t = \sum_{j=1}^{N} sgn(x_t - x_j) \quad (8)$$

Mann-Kendall test is a non-parametric statistical method that detects monotonic trends and performs mutation point identification in a dataset, by comparing the magnitude of each data point with those of all preceding observations (Mann, 1945; Kendall, 1975). For a data series x_1, x_2, ... x_n of length n:

$$S_k = \sum_{i=1}^{k} \sum_{j=1}^{i-1} sign(x_i - x_j), k = 2, 3, \dots, n \quad (9)$$

where S_k is the cumulative sum of the sign of rank differences among all data points within the first k observations. It reflects whether the current data point x_i tends to increase or decrease relative to all preceding points. The standard statistic U was then calculated:

$$UF_k = \frac{S_k - E(S_k)}{\sqrt{Var(S_k)}}, k = 1, 2, \dots, n \quad (10)$$

$$E(S_k) = \frac{k(k+1)}{4} \quad (11)$$

$$Var(S_k) = \frac{k(k-1)(2k+5)}{72} \quad (12)$$

Then, the original sequence is reversed to calculate the corresponding UB_k, which represents the trend variation from the end of the series moving backward. The intersection points of the UF_k and UB_k curves—especially within the significance range—is considered a potential change point.

https://doi.org/10.5194/egusphere-2026-296
Preprint. Discussion started: 3 February 2026

2.4 Simulation of *Rs* and soil C dynamics under future N deposition

The latest version of the Community Land Model (CLM5) (Lawrence et al., 2019a) was employed as the land modelling system, to simulate land surface processes at the global scale. The CLM5 includes comprehensive representations of bio-geophysical and bio-geochemical processes such as energy, water, and carbon-nitrogen cycling (Lawrence et al., 2019b). The CLM5 simulations are forced by the GSWP3 reanalysis data (Compo et al., 2011) product as atmospheric conditions. The International Land Atmosphere Model Benchmarking (ILAMB) project has verified that GSWP3 as the forcing data is superior to other datasets in accompanying the CLM5 when biogeochemistry is enabled (Collier et al., 2018). The N deposition experiments are conducted in the period of 1951 to 2014. Before conducting the control and sensitivity simulations, we performed a 2000-year-long spin-up simulation with the original CLM5 forced by 1950 climatological data, making the biogeochemical cycles in the model reach their equilibriums.

The CLM5 already incorporates the saturation effects of N enrichment on vegetation-related processes associated with *R*a (Lawrence et al., 2019b), and our meta-analysis indicates that the overall decline in *Rs* under excessive N addition is primarily driven by the significant reduction in *Rh* (Fig. 4). To accurately represent the effect of N-enrichment on *Rs*, we focused on modifying the *Rh* component (soil decomposition module), which results from microbial decomposition of soil organic matter and litter, while the simulation of *Ra* remained at the model's default settings. In the default model, *Rh* arises from the decomposition of soil organic matter, represented as a cascade of four soil organic matter pools (active, slow, passive, and coarse woody debris), along with three litter pools (metabolic, structural, and woody litter). Decomposition fluxes among pools are driven by base rate constants and modulated by environmental scalars for soil temperature, moisture, and mineral N availability (Lawrence et al., 2019b). These rates are further constrained by pool-specific C:N ratios and stoichiometric rules, but no explicit feedback from excess mineral N is included. To address this gap, we introduced a new soil decomposition scalar, $ndep_{scalar}$, to represent the inhibitory effect of excess soil mineral N on microbial decomposition. This scalar directly adjusts the soil decomposition fluxes: when $ndep_{scalar}$ is less than 1, it reduces the decomposition rates accordingly, thereby decreasing microbial decomposition activity and subsequently *Rh*, leading to a reduction in *Rs* (Eq. (13)). In our modification, we chose soil mineral N concentration (SNC), accumulated from atmospheric inorganic N deposition, as the N threshold indicator. Since the majority of soil mineral N is primarily concentrated in the topsoil (Fig. S1), we assumed that when the total soil mineral N of 25 soil layers is higher than N_{Th}, *Rs* was inhibited (Table S2). We implemented this relationship through the following function:

$$ndep_{scalar} = \frac{N_{Th}}{SNC} \times \alpha \quad (13)$$

where the SNC is the soil mineral N content (g m^{-2}), and α is a factor to be determined via model calibration. Ten test simulations were conducted with different α, in which α = 0 indicates that the N_{Th} is ineffective (Table S3), and the model operates identically to the default version. To calibrate the parameter α in the N scalar function (Eq. (13)), we used the fitted regression curve from the global experimental dataset (Fig. 2a) as a benchmark. For each tested value of α, we ran the model

https://doi.org/10.5194/egusphere-2026-296
Preprint. Discussion started: 3 February 2026

globally and calculated the simulated *RRs* across all grid cells and then computed the R^2 between the simulated *RRs*–N relationship and the empirical curve. The value of α that yielded the highest R^2 was selected to modify the N scalar in the CLM5, ensuring that the model better captured the empirical response pattern of *RRs* to N addition. As α increases, R^2 first increases and then decreases (Fig. S2). We therefore assumed that the "best" α could be found by applying a second-order polynomial fitting. The fitting result indicates that by theory, choosing α of 0.172 can offer the best fit between the model result and observed results from the meta-analysis (Fig. S3). Therefore, we finally chose an α of 0.172 for the model experiment in the projected period.

Given the current dataset, we can confirm that excessive N suppresses *Rs*, but we cannot robustly determine whether this suppression follows a linear or nonlinear form. While some studies have suggested potential nonlinear responses of terrestrial ecosystem to N enrichment (Janssens et al., 2010; Tian et al., 2016b), such patterns are often ecosystem-specific and require high-resolution, gradient-based, and long-term N addition experiments to detect. The available global dataset, albeit comprehensive, still lacks sufficient temporal and gradient coverage to robustly parameterize a nonlinear suppression curve. For these reasons, we retained the model's default assumption of a linear suppression effect, ensuring both simplicity and consistency with the existing CLM5 framework. We acknowledge that nonlinear responses are plausible, and incorporating such mechanisms in future work—once more targeted datasets are available—could improve the realism of model projections.

The projection scenario is set to the Shared Socioeconomic Pathway 245 and 585 (SSP245 and SSP585), implying moderate and strong global warming trends with different anthropogenic activities, respectively (Meinshausen et al., 2020). The atmospheric N deposition is also prescribed under these scenarios, the input data of which is obtained from the support model input data server of NCAR. Two cases are conducted, including one control case, which is the original CLM5 model without any N development, and one sensitivity case based on the model development with the inclusion of N_{Th}. Both cases were simulated for the period of 2015-2100, using the SSP245 or SSP585 atmospheric forcing data.

3 Results

3.1 Changes of *Rs* with N addition increase

Based on global data from 226 experiments (Fig. 1), this study shows that *Rs* remains stable up to a certain point and then declines with further N increase (Fig. 2a). The sliding t-test and Pettitt test both indicated a RR_{++} change-point at 11.3 g N m^{-2} yr^{-1}, but the Mann-Kendall test suggested a slightly higher threshold at 14 g N m^{-2} yr^{-1} (Fig. S4). Given that two independent methods consistently identified the threshold at 11.3 g N m^{-2} yr^{-1}, we considered this result more robust and adopted it as the representative change-point in this study. Therefore, we chose 11.3 g N m^{-2} yr^{-1} (90% CI: 11.28~11.52) as a key threshold for *Rs* behaviour (Figs. 2, S4). The inhibitory effects of excess N become apparent on the responses of *Rs*, mainly *Rh*, to N additions (Figs. 3, 4). This approach sheds light on the complex relationship between N addition and *Rs*, moving beyond simple low or high classifications to a more detailed understanding based on the N addition gradient.

https://doi.org/10.5194/egusphere-2026-296
Preprint. Discussion started: 3 February 2026

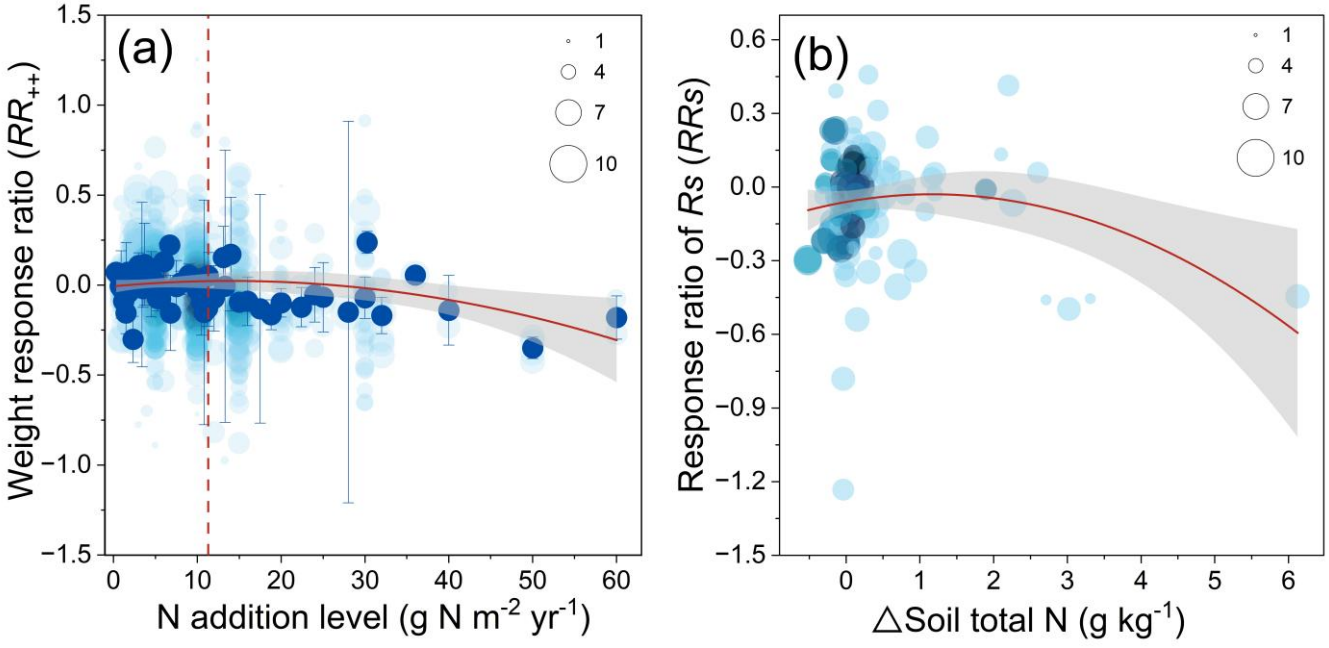

Figure 2: The changes in the weighted response ratio of soil respiration (*Rs*) (RR_{++}) with N addition gradient (a) and in the response ratio of *Rs* (*RRs*) with soil total N increments (b). The red curves represent the fitted trend (nonlinear regression), and the vertical dashed line indicates the estimated threshold identified via the change-point analysis. The dark blue dots represent the RR_{++} under each N addition level, while semi-transparent blue dots represent all observations and the size of the circles represents $\boldsymbol{ln\omega_i}$, and the shade of the dots color indicates the density of the dot distribution. The error bars and shaded areas represent the 95% confidence intervals of RR_{++} and the fitted curve, respectively.

Nitrogen addition resulted in rapid increases in soil N concentrations, and *Rs* response showed similar patterns to the increases in soil N and N addition levels (Fig. 2), highlighting the inhibitory effects of excessive N on *Rs*. In the threshold analysis, we used the absolute N addition rate to more clearly capture the response of *Rs* to N input, thereby providing a direct and practical reference for the management of anthropogenic N emissions. Besides, the background soil mineral N is negligible relative to the amount of added N (Wang et al., 2017; Wang et al., 2019). Thus, employing N addition as the basis for defining the N threshold offers a consistent and robust framework for evaluating the response of *Rs* to N enrichment.

https://doi.org/10.5194/egusphere-2026-296
Preprint. Discussion started: 3 February 2026

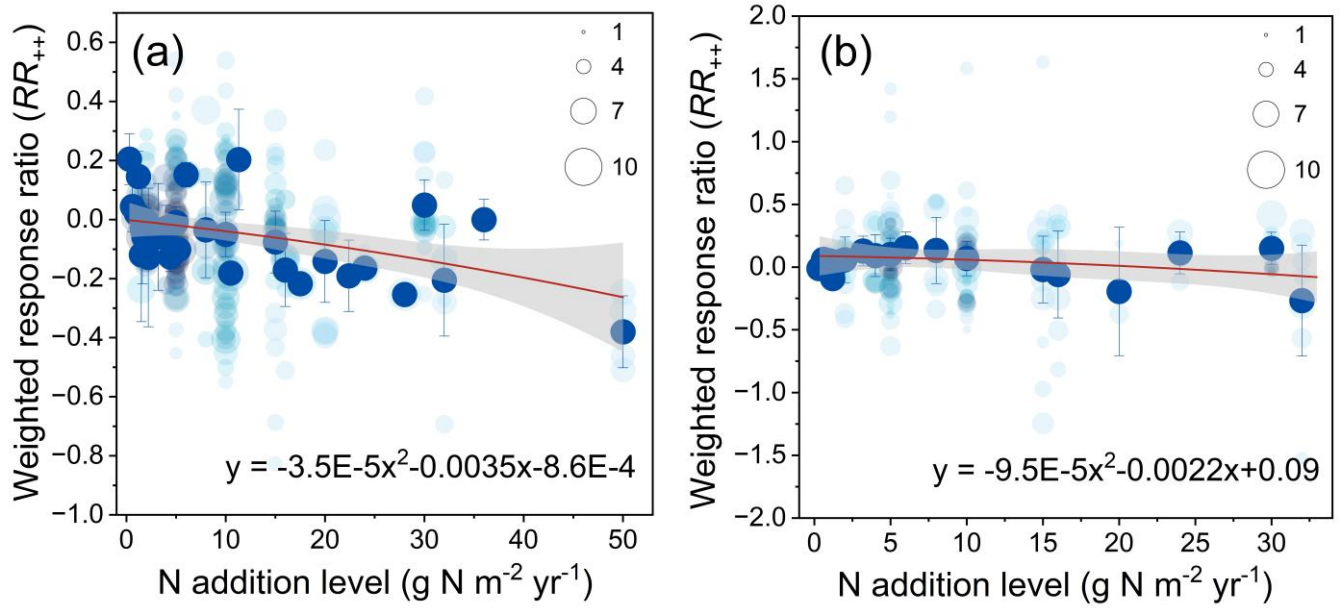

Figure 3: Weighted response of soil heterotrophic respiration (*RRh*) (a) and autotrophic respiration (*RRa*) (b) to N addition gradient. The dark blue dots represent the RR_{++} under each N addition level, the semi-transparent blue dots represent all observations and the size of the dots represents $ln\omega_i$, and the shade of the dots color indicates the density of the dot distribution. The error bars and shaded areas represent the 95% confidence intervals of RR_{++} and the fitted curve, respectively.

3.2 Responses of *Rs* and its components to N addition across ecosystems

The inhibitory effect of excessive N on *Rs* was widespread globally (Fig. 4), and was primarily driven by reductions in *Rh* (Fig. 3a, 4). Under high N addition, *Rs* and *Rh* were 9.4% (95% CI: 5.9-12.9%) and 11.3% (95% CI: 6.0-16.6%) lower than the control, respectively ($p < 0.001$) (Fig. 4a, b). In contrast, high N did not significantly affect *Ra* compared to the control, but decreased it compared to low N addition (Fig. 4c). Low N stimulated *Ra* in several ecosystems, while high N significantly suppressed *Rh* in most ecosystems. In forests, High N decreased *Rs* by 8.5% (95% CI: 4.5-12.5%, $p < 0.001$) (Fig. 4a, b), and by 14.2% (95% CI: 21.7-6.7%, $p < 0.001$) and *Rh* by 30.9% (95% CI: 38.6-23.2%, $p < 0.001$) in grasslands (Fig. 4a, b). In contrast, low N increased *Ra* by 8.6% (95% CI: 1.0-16.1%) ($p < 0.05$) in grasslands (Fig. 4c). Nitrogen addition significantly limited the plant growth in grasslands and enhanced *Ra* by increasing the aboveground net primary productivity and the belowground net primary productivity (Yan et al., 2009). However, *Rs* and its components responded negatively to high N in grasslands (Fig. 4).

For different forest ecosystems, high N significantly suppressed *Rs* across all types except temperate forests (Fig. 4a). And forests at high and low latitudes (e.g., tropical and boreal forests) tended to exhibit negative responses to both low and high N, whereas mid-latitude forests (e.g., subtropical forests and deciduous broadleaf forests) displayed stimulations under low N but suppression under high N (Fig. 4a). The *Rh* showed a weaker positive or stronger negative response to high N

https://doi.org/10.5194/egusphere-2026-296
Preprint. Discussion started: 3 February 2026

compared to low N, except for boreal forests. Plant N resorption and litter N mineralization are two major ways in which plants obtain N (Cleveland et al., 2013). Nitrogen limitation is relatively more prevalent in boreal forests and in most temperate forests (Du et al., 2020), as trees invests C for N acquisition, resulting in high C input via root exudation (Chen et al., 2014; Meyer et al., 2017), leading to a high *Rh* as a byproduct of the N-mining of soil organic matter (Deng et al., 2018). When N fertilizer occurred, N limitation of plants is alleviated, plants do not need to strongly invest more C as root exudates etc. in the rhizosphere/soil for nutrient uptake, so soil microbial activity decreases and *Rh* is drastically reduced. However, tropical forests are not N-limited, extra N input could cause nutrient imbalances (e.g., phosphorus limitations), which in turn lead to reduced root C allocation and decreased microbial activity.

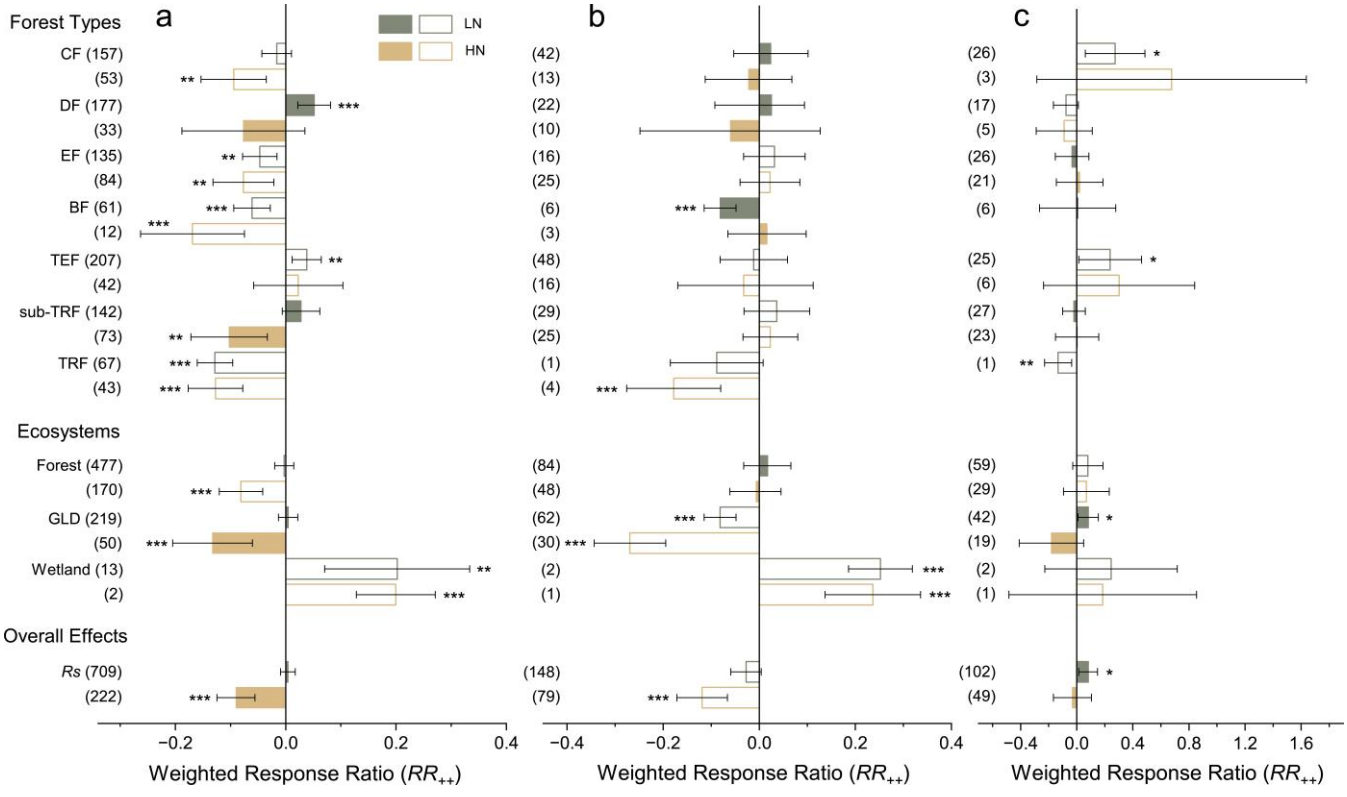

Figure 4: Weighted response ratios for total soil respiration (*Rs*) (a), heterotrophic respiration (*Rh*) (b), and autotrophic respiration (*Ra*) (c) under low (LN) and high (HN) N treatments. The acronyms CF, DF, EF, BF, TEF, sub-TRF, TRF, and GLD represent coniferous forests, deciduous broad-leaved forests, evergreen broadleaf forests, boreal forests, temperate forests, subtropical forests, tropical forests, and grasslands, respectively. Error bars represent 95% confidence intervals. The numbers in parentheses indicate the sample size while asterisks *, ** and *** denote significant effects of N addition at $p < 0.05$, $p < 0.01$, and $p < 0.001$, respectively. The filled and empty bars represent significant difference and no difference between LN and HN, respectively. The negative effects of increasing N addition were evaluated across three dimensions: (1) weakening of the positive response; (2) reversal from a positive to a negative response; and (3) strengthening of the negative response.

https://doi.org/10.5194/egusphere-2026-296
Preprint. Discussion started: 3 February 2026

3.3 Response of *Rs* under future N deposition

This study used soil mineral N concentration, the accumulation from atmospheric N deposition, as the indicator for N threshold, to revise the soil decomposition module in the CLM5 model (Methods). The CLM5 simulation results reveal that the soil mineral N has been over the threshold of 11.3 g m^{-2} long before in the high latitude regions (Fig. 5a, b). In temperate regions and the majority of the tropics, soil mineral N concentrations remain below the threshold by 2100 (Fig. 5a, b). Although anthropogenic N emissions are generally higher in mid-latitude with dense human activities, many boreal areas—including North America, Russia, and parts of the Nordic countries—have experienced higher rates of N deposition (Janssens et al., 2010; Quinn Thomas et al., 2010). Furthermore, N do not necessarily deposit locally, due to the influence of large-scale atmospheric circulation (He et al., 2025). The long-range transport and deposition of N oxides allow high-latitude regions to accumulate N more rapidly (Lee et al., 2014; Horton et al., 2015; He et al., 2025), leading to earlier exceedance of the N threshold in these areas. When soil mineral N exceeds 11.3 g m^{-2}, the relationship in the CLM5 model was adjusted by modifying the soil decomposition module (Methods). When implementing our new N scheme, the differences in *Rs* of the model projection is significant, with a maximum difference of 20% globally between the new scheme and the control one (Fig. 5c, d). The largest differences are found in the cold regions around Eurasia and North America, including Siberia, Alaska, and North Canada. Scattered regions with *Rs* inhibition also exist over northern China, southern Canada and the mid-west US, and South America (Fig. 5c, d). No significant inhibition of *Rs* by N deposition is simulated in the main tropical forests (e.g., the Central Africa forests and Amazon Rainforest) compared to boreal regions (Fig. 5c, d).

The inhibition of N deposition to *Rs* helps to store more carbon within the soil rather than it being emitted to the atmosphere, and the boreal and temperate regions contribute most, to be the major global carbon sinks (Fig. 5e, f). Based on our new model development, the current control version of the CLM5 model used in the CMIP6 project might underestimate soil carbon sequestration. Quantitatively, by the end of the 21st century, more than 15% more soil carbon sequestration in boreal regions is projected with the new model than that projected by the original model configuration (Fig. 5e, f). Nitrogen deposition is a chronic perturbation, suggesting that its effects on *Rs* may shift over time (Smith et al., 2015; Xing et al., 2022). The accumulation of soil carbon is close to linear before 2040 and starts to stabilize thereafter. By 2100, the global mean difference in soil carbon is just above 2%, implying that the inhibition of *Rs* due to the N enrichment contributes about 2% more carbon sequestration globally (Fig. 5g, h). The temporal variations of soil carbon under excessive N concentration are clearly affected by latitudes. Soil carbon accumulates rapidly at high latitudes due to stronger inhibition of *Rs* by greater N deposition rates in the boreal and temperate forests, with the difference exceeding 4% by 2100 (Fig. 5g, h). While at lower latitudes, soil carbon accumulation begins to decline around 2040 (Fig. 5g, h), this change also reflects the pattern of soil CO_2 emissions across a N addition gradient (Zheng et al., 2022).

Increased N deposition reduces soil carbon loss and promotes soil carbon sequestration, which has been demonstrated globally, especially in N-limited boreal and most temperate forests (Lu et al., 2021; Magnani et al., 2007). However, the negative impacts, including terrestrial acidification, eutrophication, and biodiversity loss, of significant reactive N deposition

https://doi.org/10.5194/egusphere-2026-296
Preprint. Discussion started: 3 February 2026

on global forests far outweigh the carbon benefits (Gundale, 2022). In addition to being harmful to terrestrial ecosystem function (Bobbink et al., 2010; Bowman et al., 2008), reactive N deposition stimulates the emissions of N_2O (Davidson, 2009) and CH_4 (Yang et al., 2022), causing a radiative forcing that can potentially offset that reduced by CO_2 sequestration (Zaehle et al., 2011). Therefore, an improved understanding of the impact of N deposition on terrestrial ecosystems and the reduction of anthropogenic N deposition is critical for mitigating climate change.

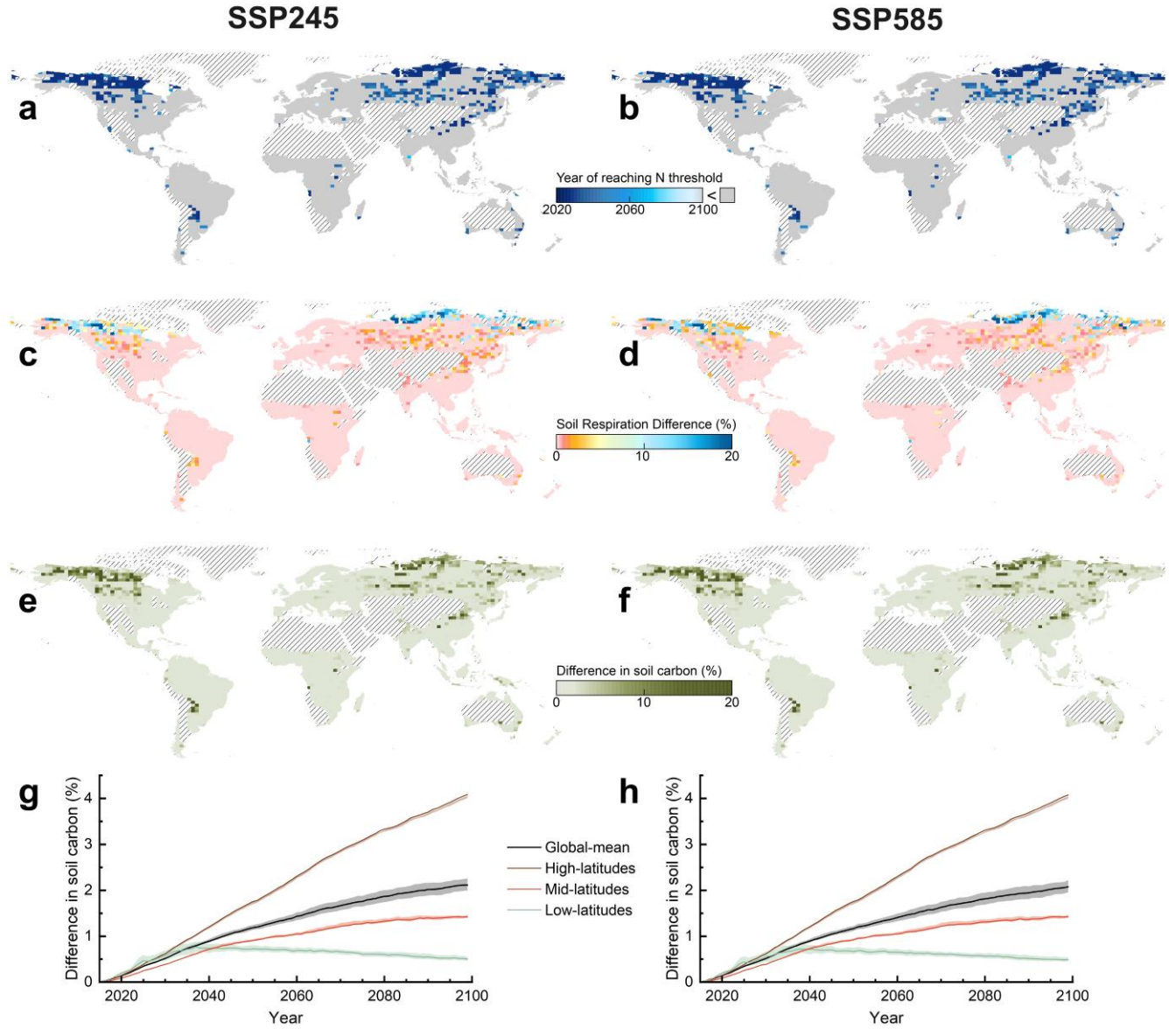

Figure 5: Global soil mineral N concentration, differences in soil respiration and soil carbon under the Shared Socioeconomic Pathway 245 and 585 (SSP245 and SSP585) scenarios by 2100. (a, b) The year when mineral N concentrations reached the N_{Th} for each grid. **(c, d)** The difference (%) in *Rs* between the sensitivity case (i.e., with N_{Th}) and the control case (i.e., without N_{Th}) by 2100. **(e, f)** The

https://doi.org/10.5194/egusphere-2026-296
Preprint. Discussion started: 3 February 2026

difference (%) in soil carbon between the sensitivity and the control cases by 2100. **(g, h)** The time series of differences in soil carbon between the sensitivity and the control cases, the shaded area represents the uncertainty of the estimates. There are no significant differences in the simulation results between the two scenarios. That is, ignoring the N-addition threshold introduces a considerable error in the estimation of *Rs* regardless of future climate change.

4 Discussion

4.1 Potential mechanism

Numerous studies have revealed the biogeochemical processes of *Rs* in response to N addition at the regional scale (Chen et al., 2017; Janssens et al., 2010; Lu et al., 2021). Here, we classified N addition into low and high N doses based on N_{Th}. The treatment is regarded as low N addition if the dose is below N_{th}, and as high N addition if the dose is above N_{th}. We further analysed the effects of different N addition levels on photosynthetic factors, vegetation growth, and soil properties, and elucidated how *Rs* responds (Figs. 4, S5). Low N addition significantly enhances photosynthesis and fine root biomass and hence *Ra* (Figs. 6, S5). However, high N addition decreases photosynthetic nitrogen-use efficiency by 40.7% (95CI%: 2.4%-79.2%) ($p < 0.01$) and decreases fine root biomass (Figs. 6, S5). Low N addition alleviates N limitation, promotes plant growth, and increases shoot biomass and the input of organic residues (Aber et al., 1998; Bai et al., 2021), while excessive N enrichment causes an imbalance of nutrients in plant tissues (Janssens et al., 2010), and reduces allocation of photosynthates from the shoot to the root system and associated mycorrhizas (Aber et al., 1998; Bond-Lamberty & Thomson, 2010), leading to decreases in root biomass and *Ra* compare to low N (Fig. 6). While plants possess the ability to regulate resource allocation in response to environmental stresses (Bloom et al.,1985), *Ra* is regulated by the plant's physiological feedback mechanisms, counteracting its decrease under high N conditions.

Low N addition has a non-significant negative effect on *Rh* (Fig. 4b), while excessive N enrichment inhibits *Rh* significantly (Fig. 4b). Generally, fertilization does not have direct effects on *Rh* (Graham et al., 2014). Excessive N addition markedly increases the concentrations of NH_4^+ and NO_3^-, and significantly decreases soil pH by 8.5% (about 0.23 pH units) (95% CI: 5.8-11.2%) ($p < 0.001$) (Figs. S5, S6). Soil acidification(Figs. 6, S5) is considered to be the main threat to soil microorganisms biodiversity (Chen et al., 2017) and a key driver of soil microbial N cycling under global change (Zhong et al., 2023). High N addition decreases microbial biomass carbon, which represents labile carbon that turns over fast in soil (Guo et al., 2020), by 8.6% (95% CI: 0.12-17.1%) ($p < 0.05$), and the diversity of arbuscular mycorrhizal fungi by 8.6% (95% CI: 7.0-10.3%) ($p < 0.01$), exacerbating the inhibition on the oxidase activity but easing the promotion on the hydrolase activity (Fig. 6). Soil microorganisms are important regulators of soil carbon emissions (Falkowski et al., 2008), playing an important role in ecosystem functions such as nutrient cycling and organic matter decomposition and their diversity is one of the key determinants of these ecological functions (Brussaard, 1997). It is shown that excessive N addition significantly decreases microbial diversity and biomass, and inhibits the production and decomposition efficiency of enzymes. These will delay the

https://doi.org/10.5194/egusphere-2026-296
Preprint. Discussion started: 3 February 2026

microbial mineralization of soil organic carbon (Lu et al., 2021), decreases the decomposition of plant litter (Michel & Matzner, 2003), and then inhibits *Rh* (Fig. 6).

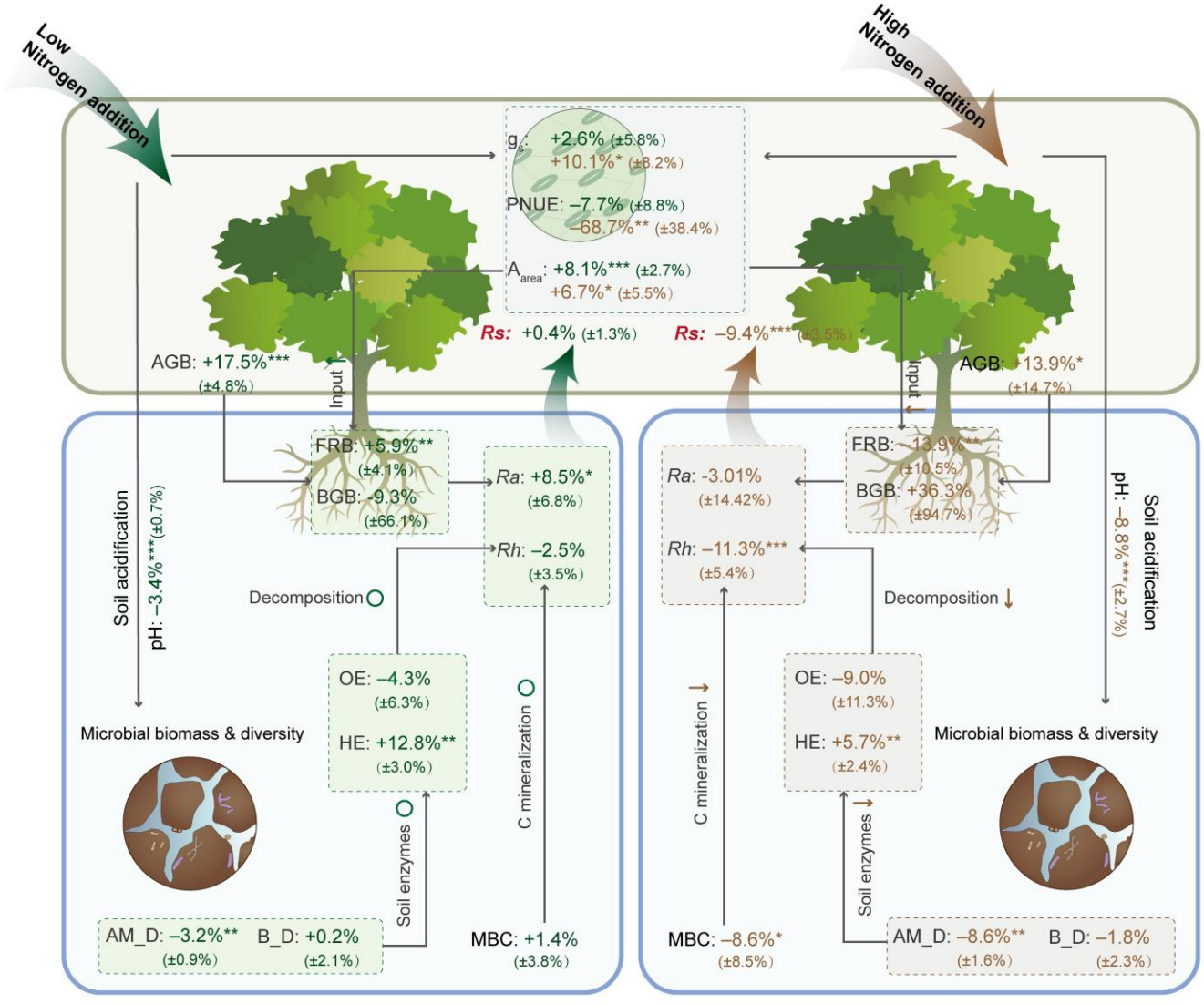

Figure 6: Potential mechanisms operating under low and high N additions, describing how increasing N addition inhibits soil respiration (*Rs*). Soil biodiversity under N enrichment was the major driver in reducing *Rs*. Heterotrophic respiration (*Rh*) rather than autotrophic respiration (*Ra*) led to the response of *Rs* under high N addition. The g_s, PNUE, A_{area}, AGB, FBC, BGB, OE, HE, AM_D, B_D, and MBC represent stomatal conductance, photosynthetic nitrogen use efficiency, photosynthetic rate per area, aboveground biomass, fine root biomass, belowground biomass, activity of oxidative enzymes, activity of hydrolytic enzymes, arbuscular mycorrhizal fungi diversity, bacterial diversity, and soil microbial biomass carbon, respectively. The green and brown numbers indicate the effects of low N addition and high N addition, and ○, *, **, *** denote not-significant effect, and significant effects at $p < 0.05$, $p < 0.01$, and $p < 0.001$, respectively. ↑ and ↓ denote significant increase and decrease, respectively.

https://doi.org/10.5194/egusphere-2026-296
Preprint. Discussion started: 3 February 2026

Globally, we also conclude that *Rh* rather than *Ra* dominates the change of *Rs* induced by excess N, although differently across vegetation types. This is inconsistent with a previous conclusion that the response of *Rs* to N addition depends more on the response of *Ra*, without considering the amount of N added (Zhou et al., 2014). Zhou et al. (2014) found that the response of *Ra* to N addition was more consistent with that of *Rs*, and concluded that ecosystem-specific differences in *Rs* response were primarily driven by variations in *Ra* due to distinct plant community characteristics. In contrast, our study found that *Rh* exhibited a stronger alignment with *Rs* across different N addition levels, especially under high N additions. This discrepancy may be attributed to two key differences between the two studies. First, our analysis was based on a more recent and comprehensive global experimental dataset, including broader ecosystem coverage and more detailed measurements. Second, Zhou et al. (2014) did not separate different levels of N addition, whereas our study explicitly accounted for N addition gradients. Our approach may better capture shifts in the dominant contributors to *Rs* under increasing N input, particularly the enhanced role of *Rh* under higher N availability.

In this study, high N decreased both *Rh* and *Ra* with the decrease in *Rh* being more pronounced. This is consistent with the response to N of below-ground processes associated with *Rh* and vegetative processes associated with *Ra* (Fig. 6). Specifically, microbial activity, which drives *Rh*, shows a more sensitive response to N addition. Previous studies have shown that soil rather than tree biomass represents the main change in carbon sink under N addition in temperate and tropical forests (Lu et al., 2021; Nadelhoffer et al., 1999).

4.2 Uncertainties

Based on the experimental dataset, we find a potential global average N addition threshold (i.e., N_{Th}) which can indicate the significant changes in *Rs*. The N_{th} served as parameter references to improve CLM5 model. It is important to emphasize that our focus lies not on the precise numerical value of the threshold, but rather on the trend shift it indicates—from stimulation to suppression in *RRs*. Capturing this ecological trend is essential for introducing biologically meaningful mechanisms into land surface models, thereby enhancing their ability to simulate soil carbon dynamics under N enrichment. Nevertheless, the identification and application of such thresholds are subject to uncertainties

First, from the ecological perspective, experimental N addition cause a rapid and substantial increase in soil mineral N availability, much higher than background levels. However, in natural ecosystems, atmospheric N deposition in most regions is generally one to two orders of magnitude lower than experimental additions, and not all the N deposition are utilized in the soil. Therefore, in our CLM5 model, we used soil mineral N concentration—representing cumulative N availability—as the threshold indicator, rather than annual deposition rates which would be too low to drive meaningful changes in *Rs* over short-time scales. What needs to be emphasized is that we did not directly equate the N addition threshold from experiments to a fixed value of soil mineral N. Instead, we used the empirical *RRs*–N addition response curve as a benchmark to calibrate a parameter (α) in the model (Eq. (13)). The model adjusts how soil mineral N inhibits *Rs* when it exceeds a flexible threshold (N_{Th}). While this approach offers a tractable and biogeochemically reasonable method to link field observations to model processes, we acknowledge that it is a simplification. For instance, the actual increase in soil mineral N might be less than the

https://doi.org/10.5194/egusphere-2026-296
Preprint. Discussion started: 3 February 2026

total N added, due to factors such as leaching and denitrification. Consequently, the saturation threshold for soil mineral N concentration is expected to be lower than the experimental N addition threshold, potentially leading to an underestimation of C sequestration in some regions in CLM5.

Second, from the methodological perspective, we employed three statistical approaches—sliding t-test, Pettitt test, and Mann-Kendall test—to detect the potential threshold in *Rs* response to N addition. While the sliding t-test and Pettitt test both indicated a change-point at 11.3 g N $m^{-2}yr^{-1}$, the Mann-Kendall test suggested a slightly higher threshold at 14.0 g N m^{-2} yr^{-1}. These differences arise from the distinct detection principles of each method. Given that two independent methods—based on different statistical assumptions—consistently identified the threshold at 11.3 g N m^{-2} yr^{-1}, we considered this result more robust and adopted it as the representative change-point in this study. Nonetheless, we acknowledge that differences in data sensitivity, test assumptions, and threshold detection algorithms can introduce uncertainty. As more long-term experimental and observational data become available, the value of this threshold is likely to be refined.

Lastly, the N addition threshold likely varies across ecosystems due to differences in plant–soil–microbe interactions. Our study indicates that forests tend to exhibit higher thresholds (10.0–11.3 g N m^{-2} yr^{-1}) than grasslands (4.0–6.7 g N m^{-2} yr^{-1}) (Figs. S7, S8). However, due to the limited availability and consistency of experimental data—particularly from underrepresented regions—we were unable to derive robust, biome-specific estimates. Future efforts should prioritize the integration of more diverse field measurements and regionally calibrated simulations to better constrain ecosystem-level N thresholds. Given that the primary aim of this study is to capture the general saturation pattern of *Rs* in response to N input at the global scale and to improve the parameterization in CLM5, we adopted a simplified, globally uniform threshold. While this approach facilitates model implementation, it may lead to over- or underestimation of *Rs* suppression in specific biomes.

Taken together, the N threshold identified in this study should be interpreted as a guiding principle for model parameterization, rather than a fixed or universal value. Our primary emphasis is on the robust trend of decreasing *Rs* response with increasing N input, which reflects a general ecological pattern and provides a foundation for incorporating saturation N response functions into terrestrial biosphere models.

5 Conclusion

Our results provide new insights and improvements for predicting the fate of soil C in the future. This study addresses the general issue of how different N addition levels affect *Rs*, and identifies a N addition threshold that determines the direction of *Rs* responses. This work sheds light on the complex relationship between N addition and *Rs*, moving beyond simple low or high classifications to a more detailed understanding based on continuous N levels. Moreover, incorporating this complex relationship into Earth system models is both challenging and critical. Based on this new relationship, our modified CLM5 model elucidates that the absence of N threshold effects on *Rs* leads to significant underestimation of global soil carbon sequestration in the future. This notable discrepancy between our predictions and those of the IPCC implies that the effect of soil C emissions on climate change could be potentially over-estimated, given the high uncertainty of soil C changes in the

https://doi.org/10.5194/egusphere-2026-296
Preprint. Discussion started: 3 February 2026

future. Our study also highlights that this new mechanism is necessary and critical for improving the predictability of Earth system models.

Code availability

Code for meta-analysis, sliding t-test, Pettitt test, Mann-Kendall test, and CLM5 model modification and projection are available from https://github.com/Wangdj23/SR_N.git

Data availability

The observation data from different sites used for meta-analysis are available in Data S1, and the data applied to simulate the future nitrogen and carbon dynamics was provided by CLM 5.0 from https://github.com/ESCOMP/CTSM/tree/release-clm5.0.31. The GSWP3 reanalysis data used to force the model was downloaded from https://svn-ccsm-inputdata.cgd.ucar.edu/trunk/inputdata/atm/datm7/atm_forcing.datm7.GSWP3.0.5d.v1.c170516/. The anomaly forcing for the future projections of SSP245 and SSP 585 were downloaded from https://svn-ccsm-inputdata.cgd.ucar.edu/trunk/inputdata/atm/datm7/anomaly_forcing/CMIP6-SSP2-4.5/ and https://svn-ccsm-inputdata.cgd.ucar.edu/trunk/inputdata/atm/datm7/anomaly_forcing/CMIP6-SSP5-8.5/ respectively. The prescribed atmospheric nitrogen deposition data for both historical period and SSP scenarios were obtained through https://svn-ccsm-inputdata.cgd.ucar.edu/trunk/inputdata/lnd/clm2/ndepdata/.

Supplement link

Supplementary materials: Figure S1-S8, Table S1-S3.

Dataset S1: The datasets needed to evaluate the conclusions. Sheet *Rs* & variables: Raw data used in the analysis including soil respiration, environmental variables, and geographical information. Sheet References: Published papers used to extract the raw data.

Author contributions

WS designed the research. DW collected the data and performed the analysis. LC developed the model code and performed the simulations. DW and LC co-wrote the manuscript. All authors edited and revised the manuscript.

Competing interests

At least one of the (co-)authors is a member of the editorial board of Biogeosciences.

https://doi.org/10.5194/egusphere-2026-296
Preprint. Discussion started: 3 February 2026

Disclaimer

Copernicus Publications remains neutral with regard to jurisdictional claims made in the text, published maps, institutional affiliations, or any other geographical representation in this paper. While Copernicus Publications makes every effort to include appropriate place names, the final responsibility lies with the authors. Views expressed in the text are those of the authors and do not necessarily reflect the views of the publisher.

Acknowledgements

We sincerely appreciate all the scientists who contribute their precious data for our synthesis study.

Financial support

This research was funded by the National Natural Science Foundation of China (42375110), the Chongqing Outstanding Youth Science Foundation (cstc2021jcyj-jqX0025), Doctoral Initial Project of Southwest University (SWUKR23002), the Chongqing Elite-Innovation and Entrepreneurship Demonstration team (cstc2024ycjh-bgzxm0050) and the Shennong Youth Talent Project (SNYCQN088-2023).

References

Aber, J., McDowell, W., Nadelhoffer, K., Magill, A., Berntson, G., Kamakea, M., McNulty, S., Currie, W., Rustad, L., Fernandez, I.: Nitrogen saturation in temperate forest ecosystems, BioSci., 48, 921–934, https://doi.org/10.2307/1313296, 1998.

Bai, E., Li, S., Xu, W., Li, W., Dai, W., Jiang, P.: A meta-analysis of experimental warming effects on terrestrial nitrogen pools and dynamics, New Phytol., 199, 441–451, https://doi.org/10.1111/nph.12252, 2013.

Bai, T., Wang, P., Ye, C., Hu, S.: Form of nitrogen input dominates N effects on root growth and soil aggregation: A meta-analysis, Soil Biol. Biochem., 157, 108251, https://doi.org/10.1016/j.soilbio.2021.108251, 2021.

Bassevill, M., Nikiforov, I. V.: Detection of abrupt changes: Theory and application, J. R. Stat. Soc. A. Stat., 158, 185, 1993.

Bloom, A. J., Chapin, F. S. I., Mooney, H. A.: Resource limitation in plants-an economic analogy, Annu. Rev. Ecol. Evol. S., 16, 363–392, https://doi.org/10.1146/annurev.es.16.110185.002051, 1985.

Bobbink, R., Hicks, K., Galloway, J., Spranger, T., Alkemade, R., Ashmore, M., Bustamante, M., Cinderby, S., Davidson, E., Denteneret, F., Emmett, B., Erisman, J. W., Fenn, M., Gilliam, F., Nordin, A., Pardo, L., De Vries, W.: Global assessment of nitrogen deposition effects on terrestrial plant diversity: A synthesis, Ecol. Appl., 20, 30–59, https://doi.org/10.1890/08-1140.1, 2010.

https://doi.org/10.5194/egusphere-2026-296
Preprint. Discussion started: 3 February 2026

Bond-Lamberty, B., Thomson, A.: A global database of soil respiration data, Biogeosciences, 7, 1915–1926, https://doi.org/10.5194/bg-7-1915-2010, 2010.

Bowman, W. D., Cleveland, C. C., Halada, Ĺ., Hreško, J., Baron, J. S.: Negative impact of nitrogen deposition on soil buffering capacity, Nat. Geosci., 1, 767–770, https://doi.org/10.1038/ngeo339, 2008.

Brussaard, L.: Biodiversity and ecosystem functioning in soil, Ambio, 26, 563–570, http://www.jstor.org/stable/4314670, 1977.

Chen, C. and Chen, H. Y. H.: Mapping global nitrogen deposition impacts on soil respiration, Sci. Total Env., 871, 161986, https://doi.org/10.1016/j.scitotenv.2023.161986, 2023

Chen, R., Senbayram, M., Blagodatsky, S., Myachina, O., Dittert, K., Lin, X., Kuzyakov, Y.: Soil C and N availability determine the priming effect: microbial N mining and stoichiometric decomposition theories, Global Chang. Biol., 20, 2356–2367, https://doi.org/10/1111/gcb.12475, 2014.

Chen, W., Xu, R., Hu, T., Chen, J., Zhang, Y., Cao, X., Wu, D., Wu, Y., Shen, Y.: Soil-mediated effects of acidification as the major driver of species loss following N enrichment in a semi-arid grassland, Plant and Soil, 419, 541–556, https://doi.org/10.1007/s11104-017-3367-x, 2017.

Chiwa, M., Tateno, R., Hishi, T., Shibata, H.: Nitrate leaching from Japanese temperate forest ecosystems in response to elevated atmospheric N deposition, J. For. Res., 24, 1–15, https://doi.org/10.1080/13416979.2018.1530082, 2019.

Cleveland, C. C., Houlton, B. Z., Kolby Smith, W., Marklein, A. R., Reed, S. C., Parton, W., Running, S. W.: Patterns of new versus recycled primary production in the terrestrial biosphere, Proc. Natl. Acad. Sci., 110, 12733–12737, https://doi.org/10.1073/pnas.1302768110, 2013.

Collier, N., Hoffman, F. M., Lawrence, D. M., Keppel-Aleks, G., Koven, C. D., Riley, W. J., Mu, M., Randerson, J. T.: The International Land Model Benchmarking (ILAMB) System: Design, theory, and implementation, J. Adv. Model. Earth Syst., 10, 2731–2754, https://doi.org/10.1029/2018MS001354, 2018.

Compo, G. P., Whitaker, J. S., Sardeshmukh, P. D., Matsui, N., Allan, R. J., Yin, X., Gleason, B. E., Vose, R. S., Rutledge, G., Bessemoulin, P., Brönnimann, S., Brunet, M., Crouthamel, R. I., Grant, A. N., Groisman, P. Y., Jones, P. D., Kruk, M. C., Kruger, A. C., Marshall, G. J., Maugeri, M., Mok, H. Y., Nordli, Ø., Ross, T. F., Trigo, R. M., Wang, X. L., Woodruff, S. D., Worleyet S. J.: The Twentieth Century Reanalysis Project, Q. J. Roy. Meteor. Soc., 137, 1–28, https://doi.org/10.1002/qj.776, 2011.

Davidson, E. A.: The contribution of manure and fertilizer nitrogen to atmospheric nitrous oxide since 1860, Nat. Geosci., 2, 659–662, https://doi.org/10.1038/ngeo608, 2009.

De Marco, A., Proietti, C., Cionni, I., Fischer, R., Screpanti, A., Vitale, M.: Future impacts of nitrogen deposition and climate change scenarios on forest crown defoliation, Environ. Poll., 194, 171–180, https://doi.org/10.1016/j.envpol.2014.07.027, 2014.

Deng, M., Liu, L., Jiang, L., Liu, W., Wang, X., Li, S., Wang, B.: Ecosystem scale trade-off in nitrogen acquisition pathways, Nat. Ecol. Evol., 2, 1724–1734, https://doi.org/s41559-018-0677-1, 2018.

https://doi.org/10.5194/egusphere-2026-296
Preprint. Discussion started: 3 February 2026

Deng, L., Huang, C., Kim, D., Shangguan, Z., Wang, K., Song, X., Peng, C.: Soil GHG fluxes are altered by N deposition: New data indicate lower N stimulation of the N_2O flux and greater stimulation of the calculated C pools, Global Chang. Biol., 26, 2613–2629, https://doi.org/10.1111/gcb.14970, 2020.

Du, E., Terrer, C., Pellegrini, A. F. A., Ahlström, A., van Lissa, C. J., Zhao, X., Jackson, R. B.: Global patterns of terrestrial nitrogen and phosphorus limitation, Nat. Geosci., 13, 221–226, https://doi.org/s41561-019-0530-4, 2020.

Falkowski, P. G., Fenchel, T., Delong, E. F.: The microbial engines that drive earth's biogeochemical cycles, Science, 320, 1034–1039, https://doi.org/10.1126/science.1153213, 2008.

Graham, S. L., Hunt, J. E., Millard, P., McSeveny, T., Tylianakis, J. M., Whitehead, D.: Effects of soil warming and nitrogen addition on soil respiration in a New Zealand Tussock grassland, PLoS ONE, 9, e91204, https://doi.org/10.1371/journal.pone.0091204, 2014.

Gundale, M. J.: The impact of anthropogenic nitrogen deposition on global forests: Negative impacts far exceed the carbon benefits, Global Chang. Biol., 28, 690–692, https://doi.org/10.1111/gcb.15959, 2022.

Guo, Z., Wang, Y., Wan, Z., Zuo, Y., He, L., Li, D., Yuan, F., Wang, N., Liu, J., Song, Y., Song, C., Xu, X.: Soil dissolved organic carbon in terrestrial ecosystems: Global budget, spatial distribution and controls, Global Ecol. Biogeogr., 29, 2159–2175, https://doi.org/10.1111/geb.13186, 2020.

He, Q., Yang, R., Gentine, P., Chen, S., Cai, L., Shi, W.: Atmospheric circulation impacts on terrestrial atmospheric nitrogen deposition under growing imbalance of regional nitrogen emissions and deposition, J. Geophys. Res-Atmos., 130, e2024JD042988, https://doi.org/10.1029/2024JD042988, 2025.

Hedges, L. V., Gurevitch, J., Curtis, P. S.: The meta-analysis of response ratios in experimental ecology, Ecology, 80, 1150–1156, https://doi.org/10.2307/177062, 1999.

Horton, D. E., Johnson, N. C., Singh, D., Swain, D. L., Rajaratnam, B., Diffenbaugh, N. S.: Contribution of changes in atmospheric circulation patterns to extreme temperature trends, Nature, 522, 465–469, https://doi.org/10.1038/nature14550, 2015.

IPCC. 2023. Climate Change 2021 – The Physical Science Basis: Working Group I Contribution to the Sixth Assessment Report of the Intergovernmental Panel on Climate Change (1st ed.). Cambridge University Press.

Janssens, I. A., Dieleman, W., Luyssaert, S., Subke, J. A., Reichstein, M., Ceulemans, R., Ciais, P., Dolman, A. J., Grace, J., Matteucci, G., Papale, D., Piao, S., Schulze, E. D., Tang, J., Law, B. E.: Reduction of forest soil respiration in response to nitrogen deposition, Nat. Geosci., 3, 315–322, https://doi.org/10.1038/ngeo844, 2010.

Kendall, M. G.: Rank Correlation Methods. Griffin, London, 1975.

Kicklighter, D. W., Melillo, J. M., Monier, E., Sokolov, A. P., Zhuang, Q.: Future nitrogen availability and its effect on carbon sequestration in Northern Eurasia, Nat. Commun., 10, 3024, https://doi.org/10.1038/s41467-019-10944-0, 2019.

Lamarque, J. F., Kiehl, J. T., Brasseur, G. P., Butler, T., Cameron-Smith, P., Collins, W D., Collin,s W. J., Granier, C., Hauglustaine. D., Hess, P. G., Holland, E. A., Horowitz, L., Lawrence, M. G., McKenna, D., Merilees, P., Prather, M. J., Rasch, P. J., Rotman, D., Shindell, D., Thornton P.: Assessing future nitrogen deposition and carbon cycle feedback using a

https://doi.org/10.5194/egusphere-2026-296
Preprint. Discussion started: 3 February 2026

multimodel approach: Analysis of nitrogen deposition, J. Geophys. Res-Atmos., 110, 2005JD005825, https://doi.org/10.1029/2005JD005825, 2005.

Lamptey, S., Li, L., Xie, J.: Impact of nitrogen fertilization on soil respiration and net ecosystem production in maize. Plant, Soil Environ., 64, 353–360, https://doi.org/10.17221/217/2018-PSE, 2018.

Lawrence, D. M., Fisher, R. A., Koven, C. D., Oleson, K. W., Swenson, S. C., Bonan, G., Collier, N., Ghimire, B., van Kampenhout, L., Kennedy, D., Kluzek, E., Lawrence, P. J., Li, F., Li, H., Lombardozzi, D., Riley, W. J., Sacks, W. J., Shi, M., Vertenstein, M., Wieder, W. R., Xu, C., Ali, A. A., Badger, A. M., Bisht, G., van den Broeke, M., Brunke, M. A., Burns, S. P., Buzan, J., Clark, M., Craig, A., Dahlin, K. Drewniak, B., Fisher, J. B., Flanner, M., Fox, A. M., Gentine, P., Hoffman, F., Keppel-Aleks, G., Knox, R., Kumar, S., Lenaerts, J., Ruby Leung, L., Lipscomb, W. H., Lu, Y., Pandey, A., Pelletier, J. D., Perket, J., Randerson, J. T., Ricciuto, D. M., Sanderson, B. M., Slater, A., Subin, Z.M., Tang, J., Quinn Thomas, R., Val Martin, M., Zeng, X.: The Community Land Model Version 5: Description of new features, benchmarking, and impact of forcing uncertainty, J. Adv. Model. Earth Syst., 11, 4245–4287, https://doi.org/10.1029/2018MS001583, 2019a.

Lawrence, D. M., Fisher, R. A., Koven, C. D., Oleson, K. W., Swenson, S. C., Vertenstein, M., Andre, B., Bonan, G., Ghimire, B., van Kampenhout, L.: Technical description of version 5.0 of the Community Land Model (CLM) (NCAR/TN-514+STR), National Center for Atmospheric Research, https://doi.org/10.1029/2018MSOO1583, 2019b.

Lee, K. H., Jose, S.: Soil respiration, fine root production, and microbial biomass in cottonwood and loblolly pine plantations along a nitrogen fertilization gradient, Forest Ecol. Manag., 185, 263–273, https://doi.org/10.1016/S0378-1127(03)00164-6, 2003.

Liang, G. P., Cai, A. D., Wu, H. J., Wu, X. P., Houssou, A. A., Cai, D. X.: Soil biochemical parameters in the rhizosphere contribute more to changes in soil respiration and its components than those in the bulk soil under nitrogen application in croplands, Plant Soil, 435, 111–125, https://doi.org/10.1007/s11104-018-3886-0, 2019.

Liu, Y., Men, M., Peng, Z., Chen, H. Y. H., Yang, Y., Peng, Y.: Spatially explicit estimate of nitrogen effects on soil respiration across the globe, Global Chang. Biol., 29, 3591–3600, https://doi.org/10.1111/gcb.16716, 2023.

Lu, M., Zhou, X., Luo, Y., Yang, Y., Fang, C., Chen, J., Li, B.: Minor stimulation of soil carbon storage by nitrogen addition: A meta-analysis, Agr. Ecosyst. Environ., 140, 234–244, https://doi.org/10.1016/j.agee.2010.12.010, 2011.

Lu, X., Vitousek, P. M., Mao, Q., Gilliam, F. S., Luo, Y., Turner, B. L., Zhou, G., Mo, J.: Nitrogen deposition accelerates soil carbon sequestration in tropical forests, Proc. Natl. Acad. Sci., 118, e2020790118, https://doi.org/10.1073/pnas.2020790118, 2021.

Magnani, F., Mencuccini, M., Borghetti, M., Berbigier, P., Berninger, F., Delzon, S., Grelle, A., Hari, P., Jarvis, P. G., Kolari, P., Kowalski, A. S., Lankreijer, H, Law, B. E., Lindroth, A., Loustau, D., Manca, G., Moncrieff, J. B., Rayment, M., Tedeschi, V., Valentini, R., Grace, J.: The human footprint in the carbon cycle of temperate and boreal forests, Nature, 447, 849–851, https://doi.org/10.1038/nature05847, 2007.

Mann, H. B.: Nonparametric tests against trend, Econometrica, 13, 245–259, https://doi.org/10.2307/1907187, 1945.

https://doi.org/10.5194/egusphere-2026-296
Preprint. Discussion started: 3 February 2026

Meinshausen, M., Nicholls, Z. R. J., Lewis, J., Gidden, M. J., Vogel, E., Freund, M., Beyerle, U., Gessner, C., Nauels, A., Bauer, N., Canadell, J. G., Daniel, J. S., John, A., Krummel, P. B., Luderer, G., Meinshausen, N., Montzka, S. A., Rayner, P. J., Reimann, S., Smith, S. J., van den Berg, M., Velders, G. J. M., Vollmer, M. K., Wang, R. H. J.: The shared socio-economic pathway (SSP) greenhouse gas concentrations and their extensions to 2500, Geosci. Model Dev., 13, 3571–3605, https://doi.org/10.5194/gmd-13-3571-2020, 2020.

Meyer, N., Welp, G., Bornemann, L., Amelung, W.: Microbial nitrogen mining affects spatio-temporal patterns of substrate-induced respiration during seven years of bare fallow, Soil Biol. Biochem., 104. 175–184, https://doi.org/10.1016/j.soilbio.2016.10.019, 2017.

Michel, K., Matzner, E.: Response of enzyme activities to nitrogen addition in forest floors of different C-to-N ratios. Biol. Fertil. Soils, 38, 102–109, https://doi.org/10.1007/s00374-003-0622-5, 2003.

Nadelhoffer, K. J., Emmett, B. A., Gundersen, P., Kjønaas, O. J., Koopmans, C. J., Schleppi, P., Tietema, A., Wright, R. F.: Nitrogen deposition makes a minor contribution to carbon sequestration in temperate forests, Nature, 398, 145–148, https://doi.org/10.1038/18205, 1999.

Niu, S., Classen, A. T., Dukes, J. S., Kardol, P., Liu, L., Luo, Y., Rustad, L., Sun, J., Tang, J., Templer, P. H., Quinn Thomas, R., Tian, D., Vicca, S., Wang, Y., Xia, J., Zaehle, S.: Global patterns and substrate-based mechanisms of the terrestrial nitrogen cycle, Ecol. Lett., 19, 697–709, https://doi.org/10.1111/ele.12591, 2016.

Payne, R. J., Dise, N. B., Field, C. D., Dore, A. J., Caporn, S. J., Stevens, C. J.: Nitrogen deposition and plant biodiversity: past, present, and future, Front. Ecol. Environ., 15, 431–436, https://doi.org/10.1002/fee.1528, 2017.

Penuelas, J.: Decreasing efficiency and slowdown of the increase in terrestrial carbon-sink activity, One Earth, 6, 591–594, https://doi.org/10.1016/j.oneear.2023.05.013, 2023.

Pettitt, A. N.: A non-parametric approach to the change-point problem, J. R. Stat., 28, 126-135, https://www.jstor.org/stable/2346729, 1979.

Quinn Thomas, R., Canham, C. D., Weathers, K. C., Goodale, C. L.: Increased tree carbon storage in response to nitrogen deposition in the US, Nat. Geosci., 3, 13–17, https://doi.org/10.1038/ngeo721, 2010.

Raich, J. W., Schlesinger, W. H.: The global carbon dioxide flux in soil respiration and its relationship to vegetation and climate, Tellus B, 44, 81–99, https://doi.org/10.1034/j.1600-0889.1992.t01-1-00001.x, 1992.

Raposo, E., Brito, L. F., Janusckiewicz, E. R., Oliveira, L. F., Versuti, J., Assumpção, F. M., Cardoso, A. S., Siniscalchi, D., Delevatti, L. M., Malheiros, E. B., Reis, R. A., Ruggieri, A. C.: Greenhouse gases emissions from tropical grasslands affected by nitrogen fertilizer management, Agron. J., 112, 4666–4680, https://doi.org/10.1002/agj2.20385, 2020.

Reay, D. S., Dentener, F., Smith, P., Grace, J., Feely, R. A.: Global nitrogen deposition and carbon sinks, Nat. Geosci., 1, 430–437, https://doi.org/10.1038/ngeo230, 2008.

Schwede, D. B., Simpson, D., Tan, J., Fu, J. S., Dentener, F., Du, E., deVries, W.: Spatial variation of modelled total, dry and wet nitrogen deposition to forests at global scale, Environ. Poll., 243, 1287–1301, https://doi.org/10.1016/j.envpol.2018.09.084, 2018.

https://doi.org/10.5194/egusphere-2026-296
Preprint. Discussion started: 3 February 2026

Smith, M. D., La Pierre, K. J., Collins, S. L., Knapp, A. K., Gross, K. L., Barrett, J. E., Frey, S. D., Gough, L., Miller, R. J., Morris, J. T., Rustad, L. E., Yarie, J.: Global environmental change and the nature of aboveground net primary productivity responses: insights from long-term experiments, Oecologia, 177, 935–947, https://doi.org/10.1007/s00442-015-3230-9, 2015.

Shukla, S. K., Yadav, R. L., Awasthi, S. K., Gaur, A.: Soil Microbial biomass nitrogen, in situ respiration and crop yield influenced by deep tillage, moisture regimes and N nutrition in sugarcane-based system in Subtropical India, Sugar Tech, 19, 125–135, https://doi.org/10.1007/s12355-016-0442-1, 2017.

Terrer, C., Phillips, R. P., Hungate, B. A., Rosende, J., Pett-Ridge, J., Craig, M. E., van Groenigen, K. J., Keenan, T. F., Sulman, B. N., Stocker, B. D., Reich, P. B., Pellegrini, A. F. A., Pendall, E., Zhang, H., Evans, R. D., Carrillo, Y., Fisher, J. B., Van Sundert, K., Vicca Sara, Jackson, R. B.: A trade-off between plant and soil carbon storage under elevated CO_2, Nature, 591, 599–603, https://doi.org/10.1038/s41586-021-03306-8, 2021.

Thomas, R. Q., Bonan, G. B., Goodale, C. L.: Insights into mechanisms governing forest carbon response to nitrogen deposition: a model–data comparison using observed responses to nitrogen addition, Biogeosciences, 10, 3869–3887, https://doi.org/10.5194/bg-10-3869-2013, 2013.

Tian, D., Niu, S., Pan, Q., Ren, T., Chen, S., Bai, Y., Han, X.: Nonlinear responses of ecosystem carbon fluxes and water-use efficiency to nitrogen addition in Inner Mongolia grassland, Funct. Ecol., 30, 490–499, https://doi.org/10.1111/1365-2435.12513, 2016a.

Tian, D., Wang, H., Sun, J., Niu, S.: Global evidence on nitrogen saturation of terrestrial ecosystem net primary productivity, Environ. Res. Lett., 11, 024012, https://doi.org/10.1088/1748-9326/11/2/024012, 2016b.

Treseder, K. K.: Nitrogen additions and microbial biomass: A meta-analysis of ecosystem studies, Ecol. Lett., 11, 1111–1120, https://doi.org/10.1111/j.1461-0248.2008.01230.x, 2008.

Viechtbauer, W.: Conducting meta-analyses in R with the *metafor* package, J. Stat. Softw., 36, 1–48, https://doi.org/10.18637/jss.v036.i03, 2010.

Wang, J., Fu, X., Zhang, Z., Li, M., Cao, H., Zhou, X., Ni, H.: Responses of soil respiration to nitrogen addition in the Sanjiang Plain wetland, northeastern China, PLoS ONE, 14, e0211456, https://doi.org/10.1371/journal.pone.0211456, 2019a.

Wang, J., Song, B., Ma, F., Tian, D., Li, Y., Yan, T., Quan, Q., Zhang, F., Li, Z., Wang, B., Gao, Q., Chen, W., Niu, S.: Nitrogen addition reduces soil respiration but increases the relative contribution of heterotrophic component in an alpine meadow, Funct. Ecol., 33, 2239–2253, https://doi.org/10.1111/1365-2435.13433, 2019b.

Wang, Q., Zhang, W., Sun, T., Chen, L., Pang, X., Wang, Y., Xiao, F.: N and P fertilization reduced soil autotrophic and heterotrophic respiration in a young Cunninghamia lanceolata forest, Agric. For. Meteorol., 232, 66–73, https://doi.org/10.1016/j.agrformet.2016.08.007, 2017.

Xing, A., Du, E., Shen, H., Xu, L., Zhao, M., Liu, X., Fang, J.: High-level nitrogen additions accelerate soil respiration reduction over time in a boreal forest, Ecol. Lett., 25, 1869–1878, https://doi.org/10.1111/ele.14065, 2022.

Xu, M., Shang, H.: Contribution of soil respiration to the global carbon equation. J. Plant Physiol., 203, 16–28, https://doi.org/10.1016/j.jplph.2016.08.007, 2016.

https://doi.org/10.5194/egusphere-2026-296
Preprint. Discussion started: 3 February 2026

Yan, L., Chen, S., Huang, J., Lin, G.: Differential responses of auto- and heterotrophic soil respiration to water and nitrogen addition in a semiarid temperate steppe, Global Chang. Biol., 16, 2345–2357, https:/doi.org/10.1111/j.1365-2486.2009.02091.x, 2009.

Yang, M., Hou, Z., Guo, N., Yang, E., Sun, D., Fang, Y.: Effects of enhanced-efficiency nitrogen fertilizers on CH_4 and CO_2 emissions in a global perspective, Field Crops Res., 288, 108694, https://doi.org/10.1016/j.fcr.2022.108694, 2022.

Yang, Y., Li, T., Pokharel, P., Liu, L., Qiao, J., Wang, Y., An, S., Chang, S. X.: Global effects on soil respiration and its temperature sensitivity depend on nitrogen addition rate, Soil Biol. Biochem., 174, 108814, https://doi.org/10.1016/j.soilbio.2022.108814, 2022.

Yu, Q., Duan, L., Yu, L., Chen, X., Si, G., Ke, P., Ye, Z., Mulder, J.: Threshold and multiple indicators for nitrogen saturation in subtropical forests, Environ. Pollut., 241, 664–673, https://doi.org/10.1016/j.envpol.2018.06.001, 2018.

Zaehle, S., Ciais, P., Friend, A. D., Prieur, V: Carbon benefits of anthropogenic reactive nitrogen offset by nitrous oxide emissions, Nature Geosci., 4, 601–605, https://doi.org/10.1038/ngeo1207, 2011.

Zheng, M., Zhang, T., Luo, Y., Liu, J., Lu, X., Ye, Q., Wang, S., Huang, J., Mao, Q., Mo, J., Zhang, W.: Temporal patterns of soil carbon emission in tropical forests under long-term nitrogen deposition, Nature Geosci. 15, 1002–1010, https://doi.org/10.1038/s41561-022-01080-4, 2022.

Zhong, Y., Yan, W., Shangguan, Z.: The effects of nitrogen enrichment on soil CO2 fluxes depending on temperature and soil properties, Global Ecol. Biogeogr., 25, 475–488, https://doi.org/10.1111/geb.12430, 2016.

Zhong, Y., Yan, W., Canisares, L. P., Wang, S., Brodie, E. L.: Alterations in soil pH emerge as a key driver of the impact of global change on soil microbial nitrogen cycling: Evidence from a global meta-analysis, Global Ecol. Biogeogr., 32, 145–165, https://doi.org/10.1111/geb.13616, 2023.

Zhou, L., Zhou, X., Zhang, B., Lu, M., Luo, Y., Liu, L., Li, B.: Different responses of soil respiration and its components to nitrogen addition among biomes: A meta-analysis, Global Chang. Biol., 20, 2332–2343, https://doi.org/10.1111/gcb.12490, 2014,

Zhou, L., Zhou, X., Shao, J., Nie, Y., He, Y., Jiang, L., Wu, Z., Bai, S. H.: Interactive effects of global change factors on soil respiration and its components: A meta-analysis, Global Chang. Biol., 22, 3157–3169, https://doi.org/10.1111/gcb.13253, 2016.